Contrib Mineral Petrol (1995) 122:262–274

Viorica Morogan · Sten Lindblom

Volatiles associated with the alkaline – carbonatite magmatism at Alnö, Sweden: a study of fluid and solid inclusions in minerals from the Långarsholmen ring complex

Received: 15 September 1994 / Accepted 25 July 1995

Abstract The Alnö alkaline-carbonatite complex consists in its northernmost part at Långarsholmen of a ring-type intrusion composed of pyroxenite, sövite and ijolite, emplaced in that order. The intrusion is surrounded by a breccia zone. The petrography, mineral chemistry and fluid/solid inclusion studies suggest that the ring complex and the main intrusion at Alnö have had a somewhat different magmatic evolution, implying different evolution of fluid phases also. At Långarsholmen, a mafic silicate magma started to crystallize Al-diopside of 0.11 CaTs (Tschermak's) content during a mid-crustal stage of evolution (ca. 5–6 kbar and 1175° C). At that stage, the mafic magma was coexisting with a Mg-bearing calcitic melt, recorded in the abundant inclusions, trapped by the crystallizing Al-diopside. The two immiscible melts appear to have separated at ca. 5 kbar and 1150° C, in good agreement with recent experimental studies. The silicate magma crystallized di + ap + magnetite during its ascent, and was in contact with a saline hydro-carbonic fluid trapped as inclusions in diopside (di) and apatite (ap) (type B2 inclusions reluctant to dissolution up to 550° C). As P_{H_2O} started to increase, Fe-pargasite began to replace the pyroxene. It appears that the fluid present at that stage was aqueous and contained ca. 40% NaCl. With decreasing *PT*, the fluid separated into two immiscible phases of high- and low-salinity (type B1 of 65% NaCl and Cl of 7% NaCl), respectively. At the shallow depths of the final emplacement, the composition of the fluid phase was most probably controlled by supply of meteoric water as indicated by the dilution trend of some B1 type inclusions. After separation, the carbonatite magma fractionated calcite + ap + dol (as shown by dolomite inclusions in early crystallizing apatite). Around 4 kbar, a CO_2-bearing aqueous fluid of low salinity ($d = 0.85$) was coexisting with the melt, and became trapped in the apatite formed during the mid-crustal stage (type A1 fluid inclusions). The residual melt was emplaced into the shallow crust and gave rise to phlogopite-bearing sövite. Fluid inclusions (type A2) trapped in calcite and in recrystallized apatite indicate that the fluid phase evolved towards a late (Na + K) hydro-carbonic fluid during cooling at the shallow depths of the final emplacement. The ijolite does not show signs of liquid immiscibility with the sövite at Långarsholmen, and exhibits mostly post-magmatic activity of fluid phases.

V. Morogan (✉) · S. Lindblom
Department of Geology and Geochemistry, Stockholm University, S-106 91 Stockholm, Sweden

Editorial responsibility: J. Touret

Introduction

The importance of volatile components during the generation, emplacement, and crystallization of carbonatites and alkaline rocks has been mentioned by many authors. According to experimental evidence, partial melting processes postulated to generate parental magmas to the alkaline-carbonatite rocks are dependent on the presence of volatile-bearing minerals and/or a free fluid phase in the mantle (Mysen and Boettcher 1975; Wyllie 1980; Olafson and Eggler 1983). Fluid interaction and metasomatism in the mantle have been reported by Menzies and Wass (1983), and Andersen et al. (1984). Furthermore, the volatiles play a major role in the evolution of alkaline silicate and carbonatite magmas, both during fractionation (Wyllie 1980) and emplacement (Andersen and Qvale 1986). Ultimately, the fluids expelled from cooling ijolite and carbonatite magmas are important for the mobilization and transport of chemical components, including REE during the fenitization process (Morogan 1989, 1994).

Although a consensus has been reached that carbonatites and the associated alkaline rocks are comagmatic and mantle derived, the genesis of carbonatites

remains controversial, being variously attributed to: (1) direct partial melting of the mantle (Eggler 1978; Koster van Gross 1975; Nelson et al. 1988; Gittins 1989; Yaxley et al. 1991); (2) fractional crystallization from carbonated silicate parental melts (Wyllie 1987); or (3) liquid immiscibility of carbonate-silicate melts (Le Bas 1989; Andersen 1986). Additional uncertainities regarding the genesis of alkaline-carbonatite complexes are the identification of parental magmas (Eggler 1978; Wyllie 1978; Edgar 1987) and the fractionation processes undergone by the magmas during their ascent to shallow levels.

Fluid inclusion studies in alkaline-carbonatite complexes are relatively few considering the role played by volatiles during the evolution of this magmatic association (Roedder 1984; Andersen 1986). According to Andersen (1984, 1986), carbonatites are highly susceptible to post-magmatic alteration, apatite appearing to be the only mineral able to survive and to retain at least partly its content of primary inclusions. Therefore, most of the inclusion studies of alkaline-carbonatite complexes deal with apatite. Roedder (1973), described CO_2-rich saline aqueous inclusions in apatite from the Amba Dongar carbonatite (India), and Rankin (1975) reported similar inclusions in apatite from the Wasaki carbonatite (Kenya). Nesbitt and Kelly (1977) found inclusion evidence that the carbonatite magma coexisted with a low-density CO_2 volatile phase at Magnet Cove (Arkansas). Primary inclusions of magmatic carbonate material in apatite have been described by Aspden (1980) from an ijolite pegmatite at Alnö, and by Ting et al. (1994) from the Sukulu carbonatite (Uganda). Andersen (1986) has documented inclusions of calcite, dolomite and devitrified mafic silicate glass, and of CO_2-bearing aqueous inclusions in apatite-rich xenoliths from the Fen carbonatite (Norway).

Fluid phases have been very active during both magmatism and fenitization at Alnö, but studies of fluid inclusions are almost completely lacking. In 1980, Aspden reported the presence of a highly alkaline aqueous solution related to a late ijolite pegmatitic stage. The study of the fluids trapped in minerals from the Alnö igneous rock series is important in order to understand the petrogenesis of this complex. Von Eckermann in his classic work (1948) interpreted the complex as being almost entirely metasomatic in origin, i.e. formed through progressive fenitization of migmatite around a carbonatitic focus, followed by instrusion of the rheomorphic fenite magma. More recently, Kresten (1979), and Morogan and Woolley (1988) have postulated a magmatic origin of the complex, and considerably reduced the area described as fenite by von Eckermann (1948, 1966). Moreover, Kresten (1979, 1990) suggested that the northernmost part of the complex, the Långarsholmen carbonatite-pyroxenite ring dyke, represents the earliest magmatic episode at Alnö. Here, we present mineral chemistry and fluid and solid inclusion data for the Långarsholmen intrusion in order to: (1) determine the nature of the fluids occurring as inclusions in minerals forming the ring-dyke rocks; (2) estimate the evolution of these fluids during the crystallization history; (3) characterize the PT-conditions during the crystallization. Furthermore, it is proposed that liquid immiscibilty between mafic silicate and carbonatite magmas was the main differentiation process.

General geology

The Alnö complex of carbonatite and alkaline rocks is located at the northern end of the Alnö Island, a few kilometres east of Sundsvall (NE Sweden) (Fig. 1). The complex was emplaced in early Proterozoic gneisses and migmatites (Kresten 1990) during the late Proterozoic – early Cambrian, with the main intrusive event at about 550 Ma (Brueckner and Rex 1980). Radiometric dating with ages ranging between ca. 610 and 530 Ma (Kresten 1990), indicate that the complex formed through repeated intrusive episodes during a time interval of ca. 80 Ma. The main complex (Alnö island) was emplaced around 546 Ma, whereas the northern ring complex at Långarsholmen intruded at about 600 Ma.

According to Kresten (1990), several intrusive centres can be recognized in the Alnö area. The main intrusion occurs on Alnö island and is subdivided into a northern ring dyke (Långarsholmen), the southern intrusion (Alnö s.s.) and the small Båräng intrusion. A breccia vent (carbonatite lapilli tuff) occurs NW of the main intrusion on Sälskär island, and another small intrusion (sövite and melilitolite) is located at Söråker on the mainland north of Alnö island. A large number of dykes (including carbonatite, alnöite and kimberlite) form a swarm that reaches up to 25 km from the main intrusion.

The main intrusion (Alnö s.s.), which is roughly circular with a diameter of about four kilometres (Fig. 1), consists of four series of igneous rocks; pyroxenite, melteigite-ijolite-urtite, nepheline syenite, and carbonatite [(silico)-sövite]. The rocks of the ijolite series dominate and the intrusion is surrounded by a fairly large fenite zone (500–600 m wide). A small sheeted intrusion of sövite occurs at Båräng, ca. 1 km W of the main complex (Fig. 1). The fenitization is less extensive in this area.

A ring intrusion of pyroxenite/sövite/ijolite occurs on the northern shore of Alnö island and the adjacent small islands, centred on Långarsholmen island (Fig. 1). According to Kresten (1990), the plutonic rocks were emplaced more or less at the same time, with the exception of an ijolite that post-dates the sövite, are probably is related to the main intrusion. The sövite and pyroxenite are intimately associated with each other. Lenticular, globular and irregular bodies with lobate margins, and veins of sövitic material occur within the silicate rocks, whereas thin layers and boudins of mafic silicate material are enclosed within the sövite, in a way that suggests liquid immiscibility. The ring complex is surrounded by a fenite breccia zone. The fenitization process in this area is less understood.

The chronological evolution of the complex according to Kresten (1979, 1980, 1990) and Morogan and Woolley (1988) can be summarized:

1. Intrusion of pyroxenite/sövite/ijolite at Långarsholmen, accompanied by fenitization and brecciation of the country rocks.
2. Intrusion of pyroxenite/ijolite (the main complex), fenitization of the country rocks and emplacement of nephelinite and phonolite dykes.
3. Intrusion of nepheline syenite (the main complex); emplacement of tinguaite and trachyte dykes.
4. Intrusion of sövite/silico-sövite (the main complex); fenitization of the host rocks.

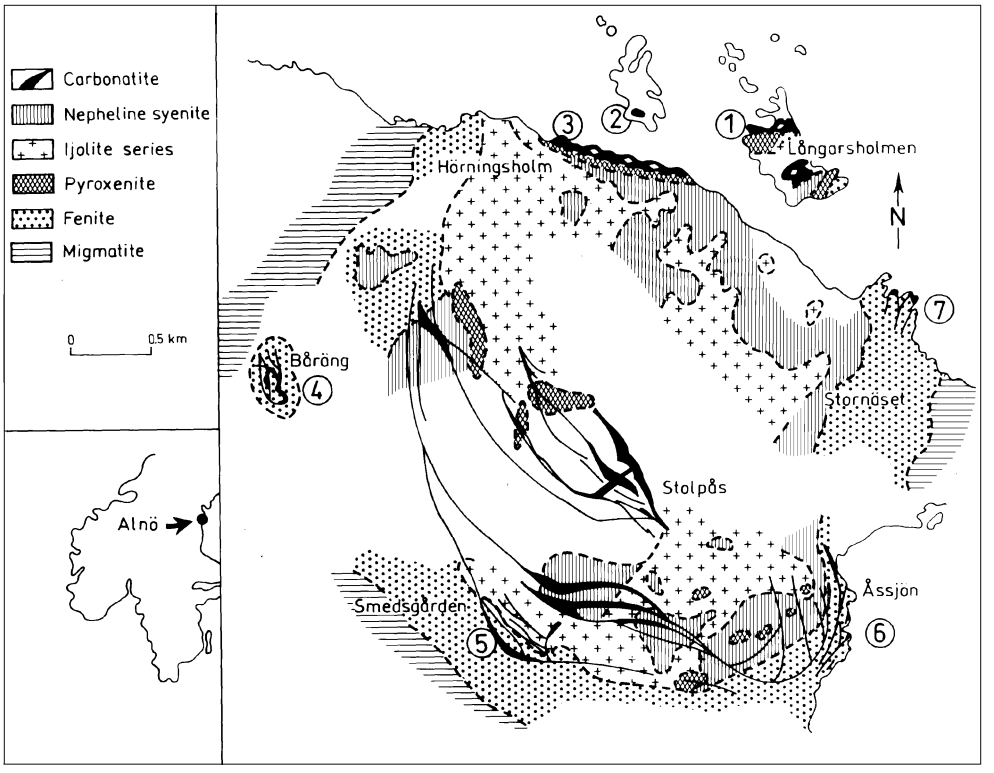

Fig. 1 Geological sketch of the Alnö complex. The numbers 1–7 indicate areas sampled for fluid inclusions studies. The ring-dyke complex (pyroxenite + sövite ± ijolite), which is the object of this article, is situated in the northernmost part (Långarsholmen area). Besides the main intrusion (pyroxenite + ijolite series + nepheline syenite + sövite dykes), a small intrusion of sövite/silico-sövite occurs at Båräng

5. Intrusion of sövite/silico-sövite at Båräng and fenitization of the country rock.
6. Emplacement of alnöite, alvikite, and beforsite dykes.

Sample description

Samples of pyroxenite, ijolite, sövite, and fenite have been collected from several sectors of the Alnö complex (Fig. 1). Since the ring complex at Långarsholmen is considered to represent the oldest magmatic event at Alnö, samples from this area have been studied using petrographic, electron microprobe and fluid inclusion techniques.

The mineralogy of the main rock types in the ring complex is summarized in Table 1. The pyroxenite and sövite contain abundant fluid inclusions in almost all mineral phases, whereas the ijolite at Långarsholmen is rather poor in fluid inclusions. The pyroxenite and sövite also contain solid inclusions of carbonate material.

Pyroxenite

The pyroxenite is a dark-coloured, medium- to coarse-grained rock (crystals up to 5 mm), with subhedral to anhedral granular texture. It consists of pyroxene (65%), apatite (20%), titanomagnetite (7%), amphibole (5%), and interstitial calcite (3%). Acicular ilmenite has been observed in pyroxene.

The main pyroxene is a pale-green diopside, containing abundant apatite and fluid inclusions. A slightly pinkish aluminian diopside occurs as corroded cores within the diopside or as agglomerates of strained crystals (undulatory extinction) surrounded by diopside. The Al-diopside contains abundant solid inclusions of carbonate (CI), and scarce inclusions of apatite.

Table 1 Mineral assemblages of the main rock types from the Långarsholmen intrusion (according to petrographic and microprobe information)

Pyroxenite[a]	Sövite[a]	Ijolite
Diopside[b]	Calcite[b]	Sodian augite
Aluminian diopside[c]	Apatite[b]	Nepheline[b]
Paragasite	Titanomagenetite	± Apatite
Titanomagnetite	± Phlogopite[b]	± Calcite
Calcite[b]	± Perovskite	± Titanomagnetite
± Biotite[b]		
± ilmenite		

[a] Rock with abundant fluid inclusions
[b] Mineral with abundant fluid inclusions
[c] Mineral with abundant solid inclusion, especially of carbonate type

Apatite occurs as elongated prisms, showing a kind of "interlocking" texture with the diopside, or as interstitial agglomerates of stout prisms. The elongated type contains solid inclusions of carbonate (CI) and scarce fluid inclusions, whereas the stout crystals are very rich in fluid inclusions. The textural relations indicate that the apatite started to crystallize early (as shown by its presence as small inclusions in Al-diopside) and continued to crystallize over a wide range of temperature, and possibly pressure.

A pargasitic amphibole replaces the diopside at a somewhat later stage of crystallization. The amphibole contains scarce fluid inclusions. Calcite occurs interstitially and encloses slender prisms of apatite and abundant fluid inclusions.

The textural relationships indicate several stages of crystallization of the pyroxenite. Earliest was Al-diopside (± apatite), then diopside + apatite + titanomagnetite crystallized, followed by amphibole (± biotite), and finally by calcite (± apatite).

Table 2 Characteristics of the fluid inclusions. A1. A2 and most of the B inclusions are primary, whereas C2, D and most of the Cl inclusions are trial-bound. See the text for further explanation regarding their textural setting

	Type A1	Type A2	Type B (B1 + B2)	Type C1	Type C2	Type D
Phases at T_{room}	$H_2O + CO_2(1)$ + vapour	$H_2O + CO_2(v + 1)$ + solids	H_2O + vapour + solids	H_2O + vapour (H_2O)	H_2O + vapour (CO_2)	One phase (H_2O/CO_2)
Shape	Tubular, irregular or negative crystal	Irregular or negative crystal	Negative crystal, or irregular tubular	Negative crystal or irregular	Tubular, negative crystal or irregular	Irregular tubular
Host mineral	Apatite	Apatite, calcite	Apatite, dioposide ± nepheline	Apatite, calcite, dioposie, nepheline, biotite	Calcite, apatite	Calcite, apatite nepheline
Host rock	Sövite	Sövite	Pyroxenite ijolite	Pyroxenite ijolite	Sövite, ± pyroxenite	Pyroxenite ijolite, sövite
Dimension	50–20 μm	50–20 μm	10–30 μm	5–30 μm	50–20 μm	2–10 μm
Illustrations	Fig. 2(A1)	Fig. 2(A2)	Fig. 2(B)	Fig. 2(C1)	Fig. 2(C2)	Fig. 2(D)

Sövite

The sövite is coarse grained (crystal size > 5 mm) and composed of calcite (85–90%), variable amounts of apatite (5–10%), titanomagnetite, phlogopite and accessory perovskite.

The calcite occurs as fairly large plates, enclosing elongated prisms of apatite and fluid inclusions. Some of the calcite has recrystallized to a mozaic of smaller grains.

The apatite forms lenses or sheaf-like agglomerates of small rounded grains, which surround elongated prisms of apatite. The latter apatite appears to have crystallized at an early stage as phenocrysts, and to have been preserved as relicts within the calcite or in the apatite agreggates. The early apatite contains solid inclusions of carbonate material and fluid inclusions, whereas the granular apatite encloses fluid inclusions only.

Ijolite

The ijolite is medium grained, with euhedral to subhedral granular texture. It consists of green sodian augite, more or less turbid nepheline, Fe-oxide, scarce interstitial calcite and accessory apatite. Nepheline is the only mineral phase containing abundant, though very small fluid inclusions. Apatite is rare and contains only a few small fluid inclusions. However, large fluid and solid inclusions in nepheline have been observed in a coarse-grained ijolite from the main intrusion (Alnö island). The rocks of the main intrusion and their inclusions will be treated elsewhere.

Fluid inclusions

Several types of fluid inclusions have been distinguished on the basis of phase relationships at room temperature and textural setting (Fig. 2). Their characteristics are listed in Table 2.

Type A inclusions are CO_2-bearing and found in sövites only (A1 and A2; Fig. 2). The A1 inclusions, which contain two liquid phases (H_2O and CO_2) and a vapour phase (CO_2), are hosted by elongated prismatic crystals of apatite, which from textural evidence is inferred to have crystallized at an early magmatic stage. The inclusions (occurring mostly as isolated inclusions and very rarely as clusters) are randomly distributed in the apatite, with their longest axis parallel to its *c* crystallographic axis. The A1 inclusions are not bound to healed fracture trails, and are considered to be primary. Moreover, when occurring close to a fracture they are empty. The A2 inclusions contain one or two liquid phases ($H_2O \pm CO_2$), a vapour phase (CO_2), and two to three solids (one or two cubic isotropic phases; halite and sylvite), and an elongated strongly birefringent phase (nahcolite, according to its Raman spectrum). The A2 inclusions are mainly hosted by the granular type of apatite, but are also found, rarely, in calcite. They show a tendency to form clusters and are not bound to healed fracture planes, also appearing to be primary.

Type B inclusions are aqueous and may contain one (B1 inclusions) or several solid phases (B2 inclusions). For simplicity, the two sub-types are treated together as type B inclusions in Fig. 2 and Table 2, but are discussed separately below. They are characteristic of the pyroxenite and some ijolites. Since the type B inclusions exhibit somewhat different morphologies and are hosted by different phases in pyroxenite compared to the ijolite, they are treated in separate columns in Fig. 2.

At room temperature, the B1 inclusions contain a liquid phase (H_2O), a vapour phase (H_2O), and a cubic isotropic solid phase (halite) of variable size. They occur only in pyroxenite, and are hosted mostly by the stout prisms of apatite. The B1 inclusions are randomly distributed or form planar arrays unrelated to healed fractures together with biphase vapour-rich C1 inclusions. The presence of two compositionally different fluid inclusions in the same domain of the host mineral suggests fluid immiscibility.

The B2 inclusions in pyroxenite consist of a liquid (L) and a vapour (V) phase and of two or three solids;

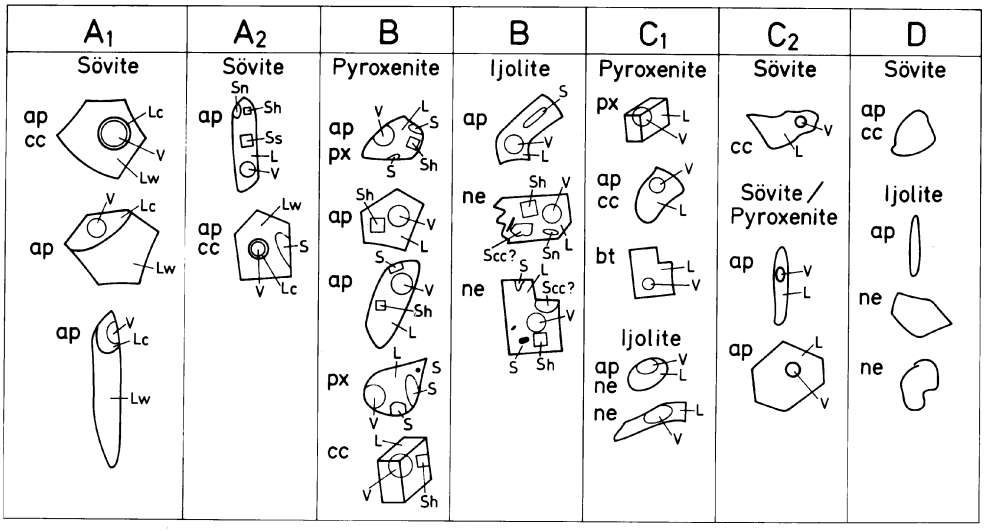

Fig. 2 Sketches of the main types of fluid inclusions. (*V* vapour, *L* liquid, *w* H_2O, *c* CO_2, *S* solid, *h* halite, *s* sylvite, *n* nahcolite, *ap* apatite, *px* pyroxene, *bt* biotite, *ne* nepheline). Note that the B type inclusions of ijolite are presented for information only since this ijolite belongs to the main intrusion

a cubic isotropic phase (halite), and one or two strongly birefringent solids (calcite and Mg-Fe carbonate according to their Raman spectra). They are hosted by diopside and the elongated prismatic apatite. The B2 inclusions are unrelated to healed fractures or cleavage planes, and occur scattered parallel to the *c*-axis of the host mineral or in clusters. The ijolite (in the main intrusion only) contains very abundant B2 inclusions enclosed in nepheline. These inclusions may contain up to five solids, generally two isotropic phases, two strongly birefringent and one opaque phase. The solid phases vary in number and size. Leakage and necking down of the B2 inclusions enclosed in nepheline is frequently observed.

The C1-biphase (V + L) and D-monophase inclusions (Fig. 2) are typically found along healed fractures and cleavage planes in almost all the constituent minerals of pyroxenite and ijolite. The C1 inclusions which are not trail bound but occur adjacent to B1 inclusions in the same mineral domain can be considered as primary and to represent an episode of fluid immiscibility (i.e. boiling). Type D inclusions of a vermicular shape are extremely abundant in the nepheline of the Långarsholmen ijolite, producing a turbid aspect to the host mineral. The C2 inclusions form secondary trails and are hosted mostly by calcite in sövite.

Solid inclusions

Solid inclusions of carbonate have been observed in both sövite and pyroxenite. The elongated prismatic apatite of sövite contains solid inclusions of dolomite of $Ca_{1.05}Mg_{0.85}Fe_{0.04}Mn_{0.02}Sr_{0.04}$ $(CO_3)_2$ composition. These inclusions (mostly single crystals) exhibit slightly rounded prismatic shape and have dimensions of 20 to 30 μm.

In the pyroxenite, A1-diopside encloses large (> 20 μm) oval or spheroidal solid inclusions of carbonate material with or without a vapour phase. These inclusions consists of a carbonate melt of magnesian calcitic composition ($Ca_{0.82}Mg_{0.12}Fe_{0.03}Mn_{0.01}Sr_{0.02}$ CO_3) trapped at a very early magmatic stage. The elongated prismatic type of apatite contains scarce inclusions of carbonate.

Microthermometry and Raman spectrometry

Phase transformations in the fluid inclusions have been studied in the temperature interval of − 120 to + 600° C, using the LINKAM THM 600 and CHAIXMECA freezing-heating stages at Oslo and Stockholm Universities. Spectra of Raman-active components have been recorded for the main types of fluid inclusions, using a multichannel Dilor Microdil XY instrument at Stockholm University. The solid inclusions were investigated at temperatures slightly above 800° C, using a LINKAM TH-1500 heating stage at Oslo University.

Results of the microthermometric observations in pyroxenite are reported in Table 3 and Fig. 3. No phase transformation, indicating the presence of CO_2 was observed in the temperature range − 80° C to the critical point of CO_2. First melting of ice (*T*m1) occurred in the interval between − 34 and − 22° C, with generation of small amounts of liquid. Larger amounts of liquid formed in the interval − 21 to − 19° C, and the last ice crystals melted between − 12 and − 5° C (*T*m2), most probably as hydrohalite. The fluid inclusions which started to melt around − 34° C may be an indication that $CaCl_2$ was present. According to Crawford (1981), Ca will lower the temperature of the first melting below − 22.8°C, which is the eutectic temperature in the H_2O-NaCl-KCl system. However, most of the inclusions started to melt around − 23° C merely indicating the presence of NaCl and possibly of KCl.

Table 3 Microthermometric data of fluid inclusions from the Långarsholmen pyroxenite. (*Tm1* temperature of the first melting, *Tm2* final melting. *Th* homogenization temperature, *Ts* dissolution temperature, *TH* total homogenization, ? the solid(s) failed to melt. *px* pyroxene)

Sample	Type	Tm1 °C	Tm2 °C	Th °C	Ts1 °C	Ts2	Ts3	Th °C	Salinity (wt %)
6/28/20	B1	− 32.8	− 5.2	349	364	–	–	364	42.9
6/28/30	B1	− 27.0	− 8.0	223	251	–	–	251	34.7
7/28/30	B1	− 24.2	− 12.2	281	339	–	–	339	40.8
6/30/20	B1(px)	–	–	386	420	–	–	420	47.9
6/30/20	B1(px)	–	–	375	410	–	–	410	47.0
6/29/30	B1	–	–	338	340	–	–	340	40.9
6/29/30	B1	–	–	442	390	–	–	442	45.1
6/29/40	B1	–	–	450	407	–	–	450	46.7
6/29/20	B1	–	–	470	345	–	–	470	41.3
7/29/10	B1	–	–	488	500	–	–	500	56.3
7/29/20	B1	–	–	553	544	–	–	553	61.5
7/29/20[a]	B1	–	–	520	515	–	–	520	58.0
8/28/25	B2	–	–	556	?	?	?	?	
8/28/25	B2	–	–	470	?	?	?	?	
7/29/10	C1	− 23.3	− 12.0	291	–	–	–	291	16.0
7/29/20[a]	C1	− 25.2	− 5.0	540	–	–	–	540	8.0
7/29/20[a]	C1	− 22.2	− 3.8	550	–	–	–	550	7.0

[a] Coeval inclusions

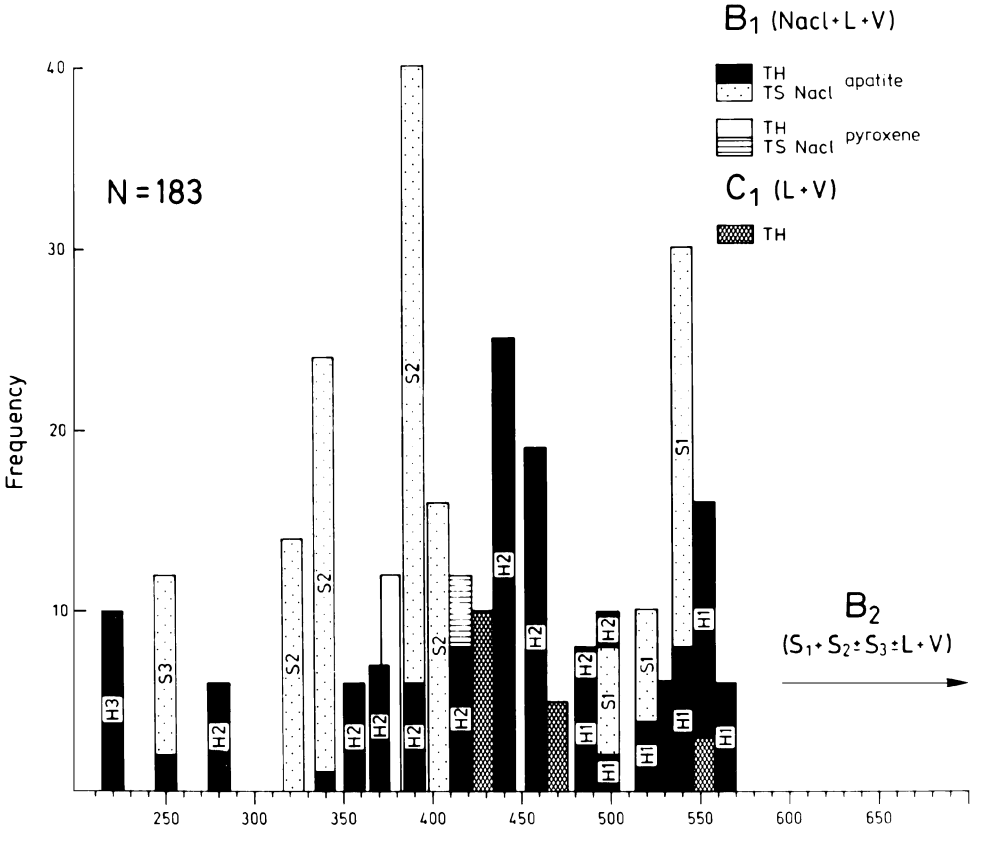

Fig. 3 Histogram of temperatures of salt dissolution (*S*) and of homogenization temperatures (*H*). The numbers *1*, *2*, and *3* refer to the main ranges of temperature exhibited by the B1 type inclusions (one solid, i.e. halite). The B1 inclusions show three intervals of maximum dissolution at 250° C, around 400° C, and between 500 and 550°C. The B2 type inclusions (with several solids) show very little dissolution. No total dissolution or homogenization has been obtained up to a ca. 550–600° C in these inclusions

During heating runs up to 550–600° C, a wide range of dissolution and homogenization temperatures were measured, as illustrated in Fig. 3. The halite-containing B1 inclusions showed several intervals of maximum dissolution of NaCl. Some secondary trail-bound B1 inclusions dissolved and homogenized around 250° C. A large number of B1 inclusions, which exhibited dissolution between 350 and 450° C, and homogenization

before, in the same interval, or after, suggest heterogeneous trapping of a saline brine (37–45 wt% NaCl equivalent). Between 500 and 550° C, the dissolution and homogenization occurred in the same range, indicating a magmatic fluid of high salinity (ca. 56–61 wt% NaCl equivalent). The biphase vapour-rich C1 inclusions homogenizing around 450–550° C are coeval with the B1 inclusions and probably related with them through immiscibility (boiling). The salinity values of Table 3 were calculated according to Potter et al. (1978) for inclusions undersaturated at room temperature, and according to Chou-Ming (1987) for the saturated ones. During heating up to 600° C, the B2-multiphase inclusions showed very little dissolution of solid phases, except for halite when present. The undissolved solids are highly birefringent and are identified as carbonates from their optical properties and Raman spectra. The most frequent carbonate has a prominent line at 1086 cm^{-1} in its Raman spectrum (Fig. 4a) corresponding to calcite (1088 cm^{-1}, Griffith 1987). Smaller anhedral inclusions exhibit lines in the range 1096–1075 cm^{-1} (Fig. 4b); they are Mg-Fe carbonates (magnesite has a characteristic line at 1096 cm^{-1} and siderite at 1071 cm^{-1}, Griffith 1987).

Results of the microthermometric observations on fluid inclusions hosted by apatite in sövite are reported in Table 4. The A1 inclusions ($L_W + L_C + V$) were studied from $-120°$ C to the critical temperature of CO_2. Melting of CO_2 was observed close to the triple point ($-56.6°$ C) , indicating that phases such as CH_4, N_2 and SO_2 (which will lower the melting temperature) were absent. This is also supported by the Raman spectra, which indicate the presence of CO_2 alone (prominent lines at 1387 and 1283 cm^{-1}). Ice started to melt around $-40°$ C but the largest amount of melt was produced close to $-20°$ C. No clathrate-hydrate formation was observed. Partial homogenization of CO_2 to gas occurred between 27 and 30° C and total homogenization to liquid in the range 260–310° C. The A2 inclusions with two or three solids were heated to homogenization. Dissolution temperatures of the solids together with microscopic observations indicate that they are sylvite, nahcolite and halite. Raman spectra of CO_2 (lines at 1387 and 1283 cm^{-1}) and nahcolite (prominent line at 1046 cm^{-1}) determined for A2 inclusions are shown in Fig. 4c and 4d, respectively.

The solid carbonate inclusions in sövite were heated up to 800–900° C but no changes could be observed. The solid inclusions in pyroxenite started to become dark when heated above 820° C, suggesting the presence of a melt.

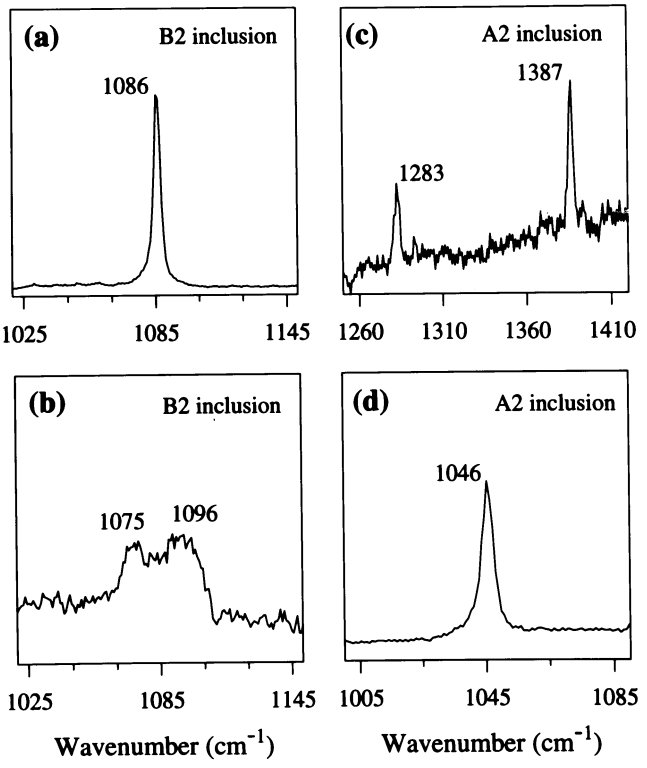

Fig. 4a–d Raman spectra of solid and liquid phases in fluid inclusions hosted in apatite from Långarsholmen pyroxenite (**a** and **b**) and sövite (**c** and **d**). **a** Calcite in primary multiphase B2 inclusion (sample 8/28/25). Lines at 712 and 281 cm^{-1} were recorded but not illustrated in the figure. **b** Mixture of Mg- and Fe-carbonates in the same inclusion as above (line at 260 cm^{-1} not illustrated). **c** CO_2 in the primary multiphase A2 inclusion (sample 1/26/10). Similar spectra of CO_2 were obtained even for the primary biphase A1 inclusions. Characteristic lines of CO_2 occur at 1388 and 1285 cm^{-1} (Van den Kerkhov 1988) **d** Nahcolite from the same inclusion. Lines which are not illustrated were recorded at 686 and 660 cm^{-1}. Characteristic lines of nahcolite are at 1048 and 684 cm^{-1} (Dhamelincourt et al. 1979).

Mineral chemistry

Major minerals in the rocks of the ring complex, and solid inclusions in apatite and pyroxene were analysed at the University of Edinburgh with a Cambridge Microscan 5 microprobe operated at 15 kv. The standards were pure elements, oxides or simple silicates. Corrections were made using computer programmes based on the methods of Sweatman and Long (1969).

Representative compositions of pyroxene are given in Table 5. In Fig. 5, which is a Q-J diagram of classification (where Q and J are Ca, Mg, Fe^{2+} and Na cations in the M (M1 + M2) sites, respectively), the pyroxenes plot in the QUAD chemical group. The pyroxene of pyroxenite is diopside, which when displaying a high-Al content can be classified as aluminian diopside. The CaTs (Tschermak's) content of the Al-diopside varies between 0.08 and 0.11 a.f.u. (atoms per formula unit), suggesting high PT-conditions of crystallization (Hertzberg 1978). In ijolite, the pyroxene is an augite, which due to a somewhat high-Na content is classified as sodian augite. The Fe and Na contents of the pyroxene, increasing from pyroxenite to ijolite

Table 4 Microthermometric data on fluid inclusions from the Långarsholmen sövite. Density calculations cf. Newitt et al. 1956; Burruss 1981; Andersen 1986. (*Ts1* dissolution of nahcolite, *Ts2* dissolution of sylvite, *Ts3* dissolution of halite, **TmC* melting of CO_2, **ThC* homogenization of CO_2, **Vc* volume CO_2; *d* density)

Sample	Type	*TmC	Tm1	Tm2	ThC	Ts1	Ts2	Ts3	TH	*V_c (vol %)	Nacl (wt %)	d (g/cm^3)
1/25/10	A1	− 55.8	− 30	− 4	+ 27.8	–	–	–	260	30	7.5	0.83
1/25/5	A1	− 57.1	− 41	− 13	+ 26.9	–	–	–	290	25	15.5	0.86
1/25/10	A1	− 56.2	− 33	− 9	± 30.0	–	–	–	310	30	13.5	0.82
1/26/10	A2					92	133	185	202			
1/26/10	A2					102	144	224	250			
1/26/5	A2					–	–	234	248			

Table 5 Representative compositions of main mineral phases from the Långarsholmen ring complex. *Di* diopside, *aug* augite, *pa* pargasite, *ph1* phlogopite)

Sample	A-6	A-6	A-6	A-5	A-6	A-6	A-6	A-1A
Rock	Pyroxenite			Ijolite	Pyroxenite			Sövite
Mineral	Al-di	Di	Al-di	Na-aug	Pa	Pa	Pa	Ph1
SiO_2	40.8	45.3	43.0	47.5	38.5	38.1	37.5	40.2
TiO_2	3.9	2.6	2.9	0.9	2.6	1.9	2.7	0.2
Al_2O_3	11.7	7.6	10.3	3.2	14.7	14.5	14.7	12.5
Cr_2O_3	0.04	0.02	0.0	0.0	–	–	–	–
FeO	10.3	9.4	9.8	11.0	13.8	14.5	12.4	5.5
MnO	0.2	0.2	0.2	0.5	0.4	0.3	0.2	0.5
MgO	8.5	10.2	9.5	8.5	11.7	11.4	12.3	25.0
CaO	23.6	23.3	23.6	19.7	11.8	12.3	12.2	0.0
Na_2O	0.5	0.7	0.4	1.1	2.3	2.4	2.3	0.1
K_2O	0.0	0.0	0.0	0.0	1.6	1.9	1.9	10.1
Total	99.5	99.3	99.8	92.4	97.6	97.3	96.2	94.1
O = 6					O = 23			O = 22
Si	1.564	1.725	1.640	1.946	5.813	5.814	5.731	5.834
Al^{IV}	0.436	0.275	0.360	0.054	2.187	2.186	2.269	2.128
Ti	0.112	0.075	0.085	0.026	0.292	0.220	0.306	0.026
Al^{VI}	0.092	0.067	0.102	0.102	0.427	0.415	0.376	0.000
Cr	0.001	0.001	0.000	0.000	–	–	–	–
Fe^{2+}	0.330	0.298	0.312	0.376	1.740	1.855	1.590	0.663
Mn	0.006	0.006	0.007	0.018	0.048	0.040	0.031	0.067
Mg	0.487	0.577	0.538	0.517	2.648	2.588	2.797	5.394
Ca	0.971	0.953	0.954	0.865	1.914	2.007	2.006	0.000
Na	0.039	0.050	0.033	0.087	0.672	0.708	0.696	0.040
K	0.000	0.000	0.000	0.000	0.368	0.375	0.374	1.872

(Table 5), suggest crystallization from genetically related magmas.

Representative analyses of amphibole are listed in Table 5. Allocation of cations and the nomenclature are according to Leake (1978). The amphiboles belong to the calcic group with $Ca_B > 1.34$, and can be classified as ferroan pargasites [$Si < 6.25$; $(Na + K)_A > 0.50$; $Ti < 0.50$; $Fe^{3+} < Al^{VI}$]. The high-Al content of the amphibole (e.g. > 2.3 a.f.u.) may indicate a temperature of crystallization around 1000°C (Helz 1973).

The solid inclusions hosted by apatite in sövite are dolomites with the composition $Ca_{1.05}Mg_{0.85}Fe_{0.04}Mn_{0.02}Sr_{0.04}(CO_3)_2$. The carbonate melt-like inclusions enclosed in the Al-diopside in pyroxenite are chemically a Mg-bearing calcite ($Ca_{0.82}Mg_{0.12}Fe_{0.03}Mn_{0.01}Sr_{0.02}CO_3$).

Discussion

Although a magmatic origin of the Alnö complex has been postulated (Kresten 1979, Morogan and Woolley 1988), the petrogenesis of the complex is still not fully understood. The nature and origin of the parental magma, the differentiation processes undergone by the ascending magma, and particularly the genesis of carbonatite magma remain to be elucidated.

The Långarsholmen ring complex and the main intrusion at Alnö appear to have had somewhat

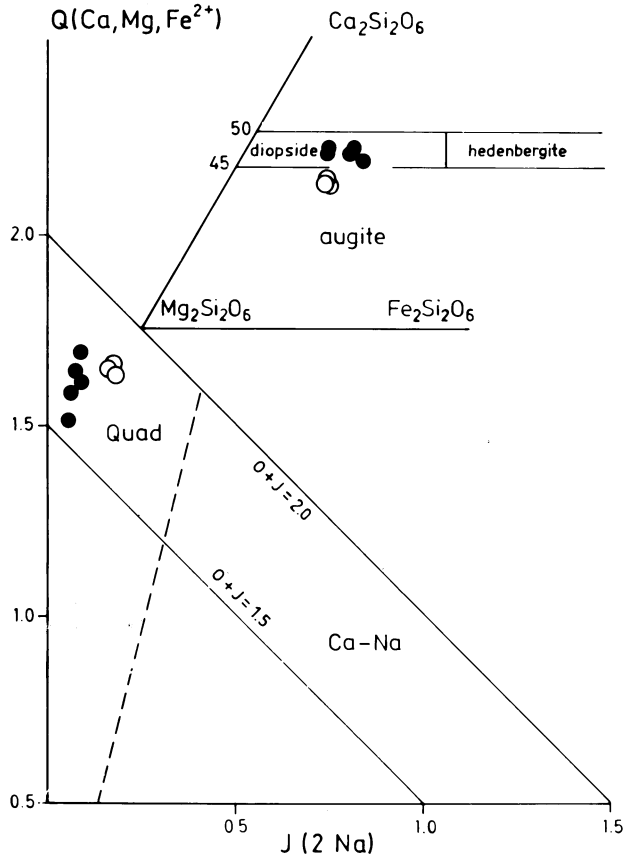

Fig. 5 Classification of pyroxene according to Morimoto (1988). (*Closed circle* pyroxene of pyroxenite, *open circle* pyroxene of ijolite)

different magmatic histories. Field relations indicate that the pyroxenite and the sövite of the ring complex are intimately related in a way suggesting liquid immiscibility. They are intruded by ijolite, which in turn is intruded by nepheline syenite. In the main complex, the silicate rocks (i.e. the pyroxenite/ijolite series and nepheline syenite) dominate and were intruded before the sövite. The latter is mainly represented as younger dykes.

The analytical results presented above show that volatiles played an important and complex role during the magmatic and post-magmatic activity at Långarsholmen. Moreover, the study of solid inclusions in the pyroxenite and sövite together with the mineral chemistry data provide important information about the differentiation and the cooling history of the complex.

The evolution of the fluid phases

Microscopic observations and microthermometric/Raman spectrometry data indicate that three generations of fluids, trapped as inclusions in minerals formed at different stages of crystallization, were present during the magmatic evolution of the Långarsholmen pyroxenite.

In Fig. 6, a plot of homogenization temperature data versus salinity outlines a complex fluid evolution in the pyroxenite during magmatic and post-magmatic stages. The multiphase B2 inclusions in diopside and apatite contain the earliest trapped fluids; these magmatic fluids were saline and carbonate rich. The coexistence of C1 and B1 inclusions in the same mineral domains, without evidence of necking down, suggests immiscibility (boiling) of an initially homogeneous fluid (ca. 40% NaCl?) above 550°C and 700 bars (phase separation in Fig. 6), and generation of a low-density low-salinity phase (salinity 7% NaCl) and a high-density high-salinity phase (salinity $>$ 60% NaCl). It appears that the original, coexisting phases were not preserved since the C1 inclusions have higher *T*H (ca. 550° C) than the corresponding B1 inclusions (ca. 520° C). Possibly, the salinity of the fluid had increased by continuous boiling, up to a value of 65% NaCl, when it became trapped at a somewhat later stage. The B1 inclusions, with salinities in the range 40–50% NaCl, may represent a cooling hypothetical fluid parental to the high-salinity inclusions (cooling trend of Fig. 6), or alternatively, the high-salinity fluid mixed with low-salinity fluids from an external source. The dilution trend displayed by some B1 inclusions in Fig. 6 was generated by mixing of late magmatic saline brines with external low-salinity waters at post-magmatic stages.

The inclusions of crystallized carbonate melt hosted by relict aluminian diopside in the pyroxenite indicate that the silicate magma was in contact with a carbonatite magma at a very early stage, when the Al-diopside crystallized. Extrapolating from the data of Hertzberg (1978), who studied the solubility of Al in clinopyroxene in undersaturated systems (e.g. gabbroic facies in the system CaO-MgO-Al_2O_3-SiO_2), the 0.1–0.08 CaTs contents of this pyroxene suggest 5–6 kbar and 1175–1275° C *PT*-conditions during its formation. The lower values seem to be a more reasonable estimation for our rocks since they display higher degree of undersaturation.

The sövite magma was in contact with two different fluids, an early CO_2-bearing aqueous fluid of low-salinity (A1 inclusions) and a late saline (Na + K) hydrocarbonic fluid (A2 inclusions). The A1 inclusions are rare and occur in apatite phenocrysts, which also contain small inclusions of dolomite. According to Wyllie (1966), carbonatite melts have eutectic temperatures as low as 625° C in the presence of a H_2O-CO_2 fluid phase. Since apatite and calcite are stable as liquidus phases over a wide range of temperatures and presures, considerations about the conditions of their formation are uncertain. Wyllie (1966) reported a minimum pressure of ca. 4 kbar for the liquidus assemblage calcite + dolomite + calcitic liquid + (H_2O-CO_2) fluid. The presence of dolomite inclusions in the apatite

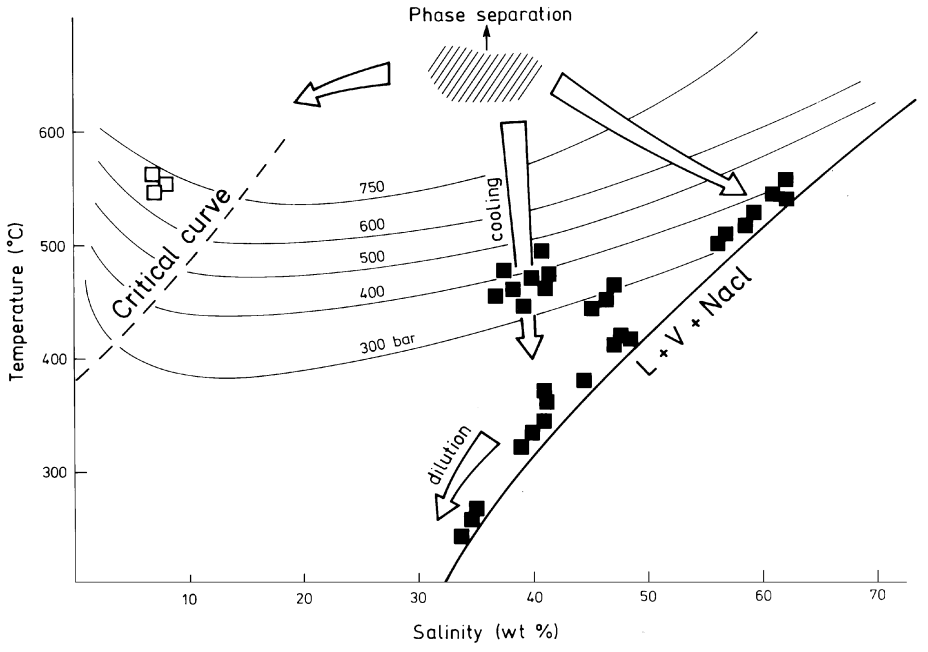

Fig. 6 *T-X* section in the system H_2O–NaCl (Sourirajan and Kennedy 1962), on which the salinities of fluid inclusions of pyroxenite are plotted. The projection of isobars for boiling conditions according to Bodnar et al. (1985). [*Open square* C1 fluid inclusions (undersaturated at T_{room}), *closed square* B1 inclusions (saturated at T_{room}]. Salinity calculations for C1 type cf. Potter et al. (1978) and for B1 type cf. Chou-Ming (1987). The *PT*-region, where hypothetically the immiscibility of an initially homogeneous fluid occurred is shown as a *shaded field*. The *arrows* illustrate possible evolutionary trends of the fluid phases coexisting with the pyroxenite at Långarsholmen

suggests that the pressure during its formation was somewhat above this value, in order to stabilize dolomite as a liquidus phase. Similar dolomite inclusions in apatite (occurring as cumulate xenoliths in carbonatite) from the Fen complex have been described by Andersen (1986), who proposed mid-crustal conditions of crystallization for the apatite and associated dolomite. Recently, Ting et al. (1994) reported the presence of Mg-calcite inclusions in early crystallized apatite from the Sukulu carbonatite in Uganda, and determined temperatures of melting for the inclusions in the range 740–912° C.

A mean isochore (density = 0.85) for the A1 inclusions was calculated according to Bowers and Helgeson (1985), and using a DENFIND programme with an empirically derived equation of state for the ternary H_2O-CO_2-NaCl system. The isochore is plotted in Fig. 7.

The A2 inclusions in sövite are enclosed in fine-grained apatite (granular aggregates), which seems to have formed at a late stage, possibly due to recrystallization of primary apatite. The late high-salinity (Na + K) hydro-carbonic fluid represented by the A2 inclusions probably became enriched in incompatible highly soluble elements during fractionation of the sövite magma. The complex composition of these inclusions precludes a calculation of isochores at the present stage of knowledge. The saline hydro-carbonic fluid may very well be responsible for the fenitization of the country rocks.

The magmatic evolution of the Långarsholmen ring-intrusion

Figure 7 is an attempt to model the evolution of the pyroxenite and sövite magmas and coexisting volatile phases at Långarsholmen, based on fluid inclusions, mineral chemistry and experimental data from the literature. As seen in the diagram, the isochore of the CO_2-bearing fluid (A1) does not cross the *PT*-box of the carbonatite (sövite) final emplacement, indicating trapping of the fluid at much higher pressure (around 4 kbar). This supports a mid-crustal origin of the apatite phenocrysts in the sövite; such an origin is independently indicated by the dolomite inclusions. Although the isochore of the A1 fluid might intersect the cooling path of sövite at very low temperatures, the textural setting of the A1 inclusions (occurring randomly distributed in the apatite, unrelated to healed fractures) supports an early magmatic, primary origin. The Al-diopside of the pyroxenite also crystallized at a mid-crustal level, most probably at a pressure of about 5 kbar, though at a higher temperature than the apatite (ca. 1200° C). The abundance of oval/spheriodal carbonate melt-like inclusions in Al-diopside (CI in Fig. 7) indicates that the mafic silicate magma was immiscibily coexisting with a carbonatite magma at the *PT*-conditions of Al-diopside crystallization. Liquid immiscibility between carbonatite and mafic silicate magmas has also been suggested by Andersen (1986) for the Fen

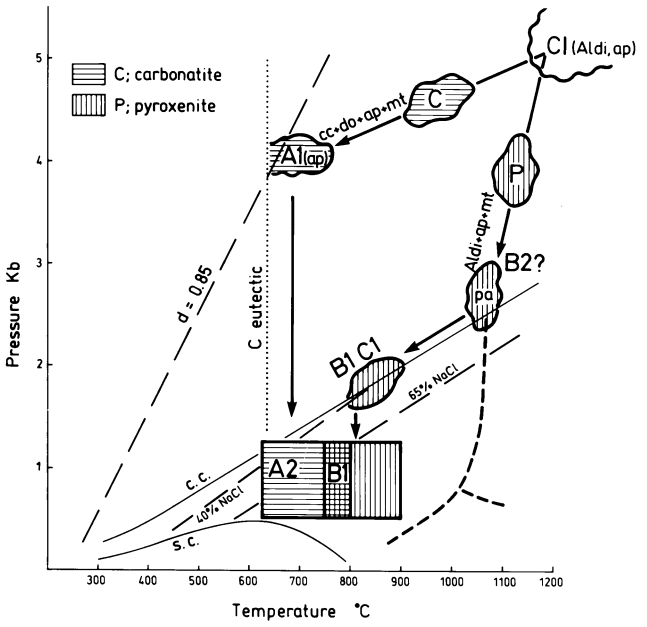

Fig. 7 Schematic magmatic evolution of the Långarsholmen ring complex and the evolution of the related fluid phases. A *PT*-region for the formation of Al-diopside containing the Mg-calcite melt-like inclusions (CI) is indicated at ca. 5 kbar and 1200° C (extrapolated from Hertzberg 1978). The *stippled line* shows the stability field of pargasite (after Westrich and Holloway 1981). A *PT*-region for the formation of apatite phenocrysts (containing dolomite inclusions) of sövite is limited by the carbonatite eutectic (ca. 625° C according to Wyllie, 1966) and by the minimum pressure for the liquidus assemblage calcite + dolomite + calcitic liquid + binary H_2O–CO_2 fluid (ca. 4 kbar, Wyllie 1966). The A1 type inclusions of sövite are represented by an isochore (*dashed line*) illustrating the mean of the encountered compositions ($H_2O_{89}CO2_6NaCl_5$) and of their density range ($d = 0.85$) . Calculations are based on Bowers and Helgeson (1985), and Bodnar (1983). The B1 inclusions of pyroxenite are represented by the 40% and 65% NaCl isopleths (*dashed lines*). The critical curve (*cc*) and the saturation curve (*sc*) are shown. The *PT*-conditions of intrusion at the present level of sövite and pyroxenite are indicated as *shaded boxes*. The assumed pressure range for final emplacement (0.5–1.5 kbar) is based on Kresten (1979). The *arrows* show the separation of the carbonatite and mafic silicate magmas through immiscibility at ca. 5 kbar and 1200° C (conforming to the Al-diopside composition enclosing the CI inclusions, and according to Kjarsgaard and Hamilton 1988), and then illustrate the cooling history as estimated from fluid inclusions and mineral chemistry data

alkaline-carbonatite complex in Norway. Moreover, an experimental study by Kjarsgaard and Hamilton (1988) demonstrated the coexistence of mafic silicate and carbonate melts at 5 kbar and 1150° C, i.e. close to the *PT*-conditions of pyroxenite and carbonatite immiscibility at Långarsholmen.

After their differentiation, the silicate and sövite magmas started to ascend and evolved separately (Fig. 7). The temperature decreased rapidly in the sövite, and at ca. 4 kbar and 750° C it was coexisting with a CO_2-bearing fluid, which was trapped in the crystallizing apatite (A1 inclusions). The partially crystallized sövite was subsequently emplaced rapidly into the shallow crust, where the apatite probably recrystallized in the presence of a highly saline hydro-carbonic fluid (A2 inclusions). The temperature of the mafic silicate magma decreased somewhat more slowly during the emplacement. The partial pressure of water increased, and at around 2 kbar and 1000° C the replacement of the pyroxene by pargasite started. Possibly, the early magmatic saline hydro-carbonic fluid (B2 inclusions in diopside and apatite) was coexisting with magma before the crystallization of pargasite. It seems that the temperature decreased more rapidly below 2 kbar, and the coexisting fluid (ca. 40% NaCl) separated into low-density (C1 inclusions) and high-density fractions (B1 inclusions), below 1.5 kbar and 800° C. An alternative explanation for the presence of a highly saline residual fluid in the pyroxenite may be removal of water from the ambient fluid phase through water-consuming reactions, i.e. replacement of pyroxene by amphibole. The isopleth of 65% NaCl (B1 inclusions) intersects the *PT*-box of final emplacement of pyroxenite in Fig. 7, suggesting that the high-salinity fluid fraction with dissolution and homogenization temperatures around 500° C was trapped during this stage. The saline fluid started to mix with low-salinity waters from external sources at late magmatic to post-magmatic stages, giving the dilution trend in Fig. 6.

The ijolite of the ring intrusion does not show signs of liquid immiscibility with the sövite magma; it mainly shows sign of interaction with post-magmatic fluids. Such fluids were present in all rock types of the Långarsholmen ring complex (type C2 and D inclusions).

Preliminary information (microscopic observations and heating runs up to 550° C) indicate that the ijolite magma of the main intrusion was in contact with a highly saline hydro-carbonic fluid (type B2 inclusions). Some solid inclusions seem to contain carbonate and/or silicate melt, which suggests that the ijolite and sövite magmas were immiscible in the main intrusion at Alnö.

Concluding remarks

1. Fluid phases were present during magmatic stages of the pyroxenite and sövite in the Långarsholmen ring complex, whereas the ijolite only was affected by post-magmatic fluids.
2. The early stage in the evolution of the pyroxenite and sövite took place in the middle crust, where carbonate melt inclusions were trapped during crystallization of aluminian diopside in the pyroxenite, and dolomite inclusions and CO_2-bearing inclusions (A1) became enclosed in apatite of the sövite.
3. Mafic silicate melt was immiscibily coexisting with Mg-bearing calcitic magma in the middle crust at a pressure of ca. 5 kbar and temperatures around 1175° C.

4. After separation of the two immiscible melts, the carbonatite magma fractionated calcite + apatite + dolomite above 4 kbar, yielding a residual liquid, which was emplaced into the shallow crust and gave rise to the phlogopite sövite. The fluid phase evolved towards a late (Na + K)-rich hydro-carbonic fluid (A2 inclusions) during the emplacement and evolution at shallow depths.
5. The mafic silicate magma fractionated Al-diopside/diopside + magnetite + apatite during its ascent and was in contact with a saline hydro-carbonic fluid (B2 inclusions). Below 2 kbar, Fe-pargasite started to replace the pyroxene. The fluid phase present at this stage was probably aqueous and of moderate salinity (approx. 40 wt% NaCl). With further decreases in pressure and temperature, the fluid split into high-salinity and low-salinity fractions (B1 and C1 inclusions, respectively). However, the B1 inclusions (65% NaCl) were trapped at a somewhat later stage, possibly after prolonged circulation of the fluid. Alternatively, the increased salinity of the fluid could be due to the crystallization of pargasite. During emplacement into the shallow crust, the composition of the residual fluid was probably modified by fluids from external sources.
6. The Långarsholmen ijolite does not show signs of liquid immiscibility with the carbonatite magma.

Acknowledgements This research was made possible by a grant to V.M. from the Swedish Council of National Research (NFR). Some of the results presented in this paper were obtained during a visit to the Mineralogical-Geological Museum, University of Oslo, under the supervision of Professor T. Andersen, whose support is gratefully acknowledged by V.M. Facilities for electron microprobe work were provided by the Department of Geology and Geophysics, University of Edinburgh. Dr. K. Broman is thanked for analytical contribution (Raman analysis) and useful discussions. This paper has benefited from valuable critical reviews by Professors T. Andersen, P. Philippot and J.L.R. Touret.

References

Andersen T (1984) Secondary processes in carbonatites: petrology of 'rödberg' (hematite-calcite-dolomite carbonatite) in the Fen central complex, Telemark (South Norway). Lithos 17:227-245

Andersen T (1986) Magmatic fluids in the Fen carbonatite complex, SE Norway: evidence of mid-crustal fractionation from solid and fluid inclusions in apatite. Contrib Mineral Petrol 93:491–503

Andersen T, Qvale H (1986) Pyroclastic mechanisms for carbonatite intrusion: evidence from intrusives in the Fen central complex, SE Norway. J Geol 94:762–769

Andersen T, O'Reilly SY, Griffin WL (1984) The trapped fluid phase in upper mantle xenoliths from Victoria Australia: implications for mantle metasomatism. Contrib Mineral Petrol 88:72–85

Aspden JA (1980) The mineralogy of primary inclusions in apatite extracted from Alnö ijolite. Lithos 13:263–268

Bodnar RJ (1983) A method of calculating fluid inclusion volumes based on vapour bubble diameters and *P-V-T-X* properties of the inclusion fluids. Econ Geol 78:535–542

Bodnar RJ, Burnham CW and Sterner SM (1985) Synthetic fluid inclusions in natural quartz: determinations of phase equilibrium properties in the system H_2O–NaCl to 1000° C and 1500 bars. Geochim Cosmochim Acta 49:1861–1873

Bowers TS, Helgeson HC (1985) Fortran programs generating fluid inclusion isochores and fugacity coefficients for the system H_2O–CO_2–NaCl at high pressures and temperatures. Comput Geosci 11:203–213

Brueckner HK, Rex DC (1980) K-A and Rb-Sr geochronology and Sr isotopic study of the Alnö alkaline complex, northeastern Sweden. Lithos 13:111–119

Burruss RC (1981) Analysis of phase equilibria C–O–H–S fluid inclusions. Mineral Assoc Can Short Course Handb, pp 39–74

Chou-Ming IM (1987) Phase relations in the system NaCl–CaCl–H_2O. III. Solubilities of halite in vapour-saturated liquidus above 445° C and redeterminations of phase equilibrium properties in the system NaCl–H_2O to 1000° C and 1500 bar. Geochim Cosmochim Acta 51:1965–1976

Crawford ML (1981) Phase equilibria in aqueous fluid inclusions. Mineral Assoc Can Short Handb 6:75–100

Dhamelincourt P, Beny JM, Dubessy J, Poty B (1979) Analyse des inclusions fluides par le microsonde Raman MOLE. Bull Minéral 102:600–610

Eckermann von H (1948) The alkaline district of Alnö Island. Sver Geol Unders Ca 36:176p

Eckermann von H (1966) Progress of research of the Alnö carbonatite. In: Tuttle GF, Gittins J (eds). Carbonatites. Interscience, New York, pp 3–31

Edgar AD (1987) The genesis of alkaline magmas with emphasis on their source regions: inferences from experimental studies. In: Fitton JG, Upton BGJ (eds) Alkaline igneous rocks. Geol Soc Spec Publ 30, pp 29–52

Eggler DH (1978) The effect of CO_2 upon partial melting of peridotite in the system Na_2O–CaO–Al_2O_3–MgO–SiO_2–CO_2 to 35 kbar, with an analysis of melting in a peridotite-H_2O–CO_2 system. Am J Sci 278:305–343

Gittins J (1989) The origin and evolution of carbonatite magmas. In: Bell K (ed) Carbonatites – genesis and evolution. London, Unwin Hyman, pp 580–600

Griffith WP (1987) Advances in the Raman and infrared spectroscopy of minerals. In: Clark RJH, Hester RE (eds) Spectroscopy of inorganic-based materials. John Wiley and Sons Ltd, London, New York pp 119–186

Helz RT (1973) Phase relations of basalts in their melting ranges at P_{H_2O} = 5 kbar as a function of oxygen fugacity. I. Mafic phases. J Petrol 80:249–302

Hertzberg CT (1978) Pyroxene geothermometry and geobarometry: experimental and thermodynamic evaluation of some subsolidus phase relations involving pyroxene in the system CaO–MgO–Al_2O_3–SiO_2. Geochim Cosmochim Acta 42:945–957

Kerkhof van den AM (1988) The system CO_2–CH_4–H_2 in fluid inclusions: theoritical modelling and geological applications. PhD thesis. Free University Press, Amsterdam

Kjarsgaard BA, Hamilton DL (1988) Liquid immiscibility and the origin of alkali-poor carbonatites. Mineral Mag 52:43–55

Koster van Gross AF (1975) The effect of high CO_2 pressure on alkalic rocks and its bearing on the formation of alkalic ultrabasic rocks and the associated carbonatites. Am J Sci 273:163–185

Kresten P (1979) The Alnö complex: discussion of the main features, bibliography and excursion guide. Nordic Carbonatite Symp

Kresten P (1980) The Alnö complex: tectonics of dyke emplacement. Lithos 13:153–158

Kresten P (1990) The Alnö area (in Swedish). In: Lundqvist T (ed) Beskrivning till bergrundskartan över Västernorrlands län. Sver Geol Unders Ba 31:pp 238–278

Leake BE (1978) Nomenclature of amphiboles. Can Mineral 16:501–520

Le Bas MJ (1989) Diversification of carbonatite. In: Bell K (ed): Carbonatites – genesis and evolution, London, Unwin Hyman, pp 428–447

Menzies MA, Wass SY (1983) CO_2 and REE-rich mantle below eastern Australia: a REE and isotopic study of alkaline magmas and apatite-rich mantle xenoliths from the Southern Highlands Province, Australia. Earth Planet Sci Lett 65:287–302

Morimoto N (1988) Nomenclature of pyroxenes. Bull Mineral 111:535–550
Morogan V (1989) Mass transfer and REE mobility during fenitization at Alnö, Sweden. Contrib Mineral Petrol 103:25–34
Morogan V (1994) Ijolite versus carbonatite as sources of fenitization. Terra nova 6(2):166–176
Morogan V, Woolley AR (1988) Fenitization in the Alnö complex, Sweden: distribution, mineralogy and genesis. Contrib Mineral Petrol 100:169–182
Mysen B and Boettcher AL (1975) Melting of a hydrous mantle. J Petrol 16:520–548; 549–593
Nelson DR, Chivac AR, Chappell BW, McCulloch MT (1988) Geochemical and isotope systematics in carbonatites and implications for the evolution of oceanic-island sources. Geochim Cosmochim Acta 52(1):1–17
Nesbitt BE, Kelly WC (1977) Magmatic and hydrothermal inclusions in carbonatite of the Magnet Cove complex, Arkansas. Contrib Mineral Petrol 63:271–294
Newitt DM, Pai MW, Kuloor NR, Hugill JAW (1956) Carbon dioxide. In: Din F (ed) Thermodynamic functions of gases, vol 1. Butterworths, London, pp 102–134
Olafson M, Eggler DH (1983) Phase relations of amphibole, amphibole-carbonate and phlogopite-carbonate peridotite: petrological constraints on the asthenosphere. Earth Planet Sci Lett 64:305–315
Potter RW, Clynne MA, Brown DL (1978) Freezing point depression of aqueous sodium chloride solutions. Econ Geol 73:284–285
Rankin AH (1975) Fluid inclusion studies in apatite from carbonatites of the Wasaki area of western Kenya. Lithos 8:123–136
Roedder E (1973) Fluid inclusions from the fluorite deposits associated with carbonatite of Amba Dongar, India and Okorusu, South West Africa. Inst Min Metall Trans B 82:835–839
Roedder E (1984) Fluid inclusions. (Reviews in mineralogy 12) Mineral Soc Am, Washington, DC
Sourirajan S, Kennedy GC (1962) The system H_2O–NaCl at elevated temperatures and pressures. Am J Sci 260:115–141
Sweatman TR, Long JVP (1969) Quantitative electron microanalysis of rock-forming minerals. J Petrol 10:332–379
Ting W, Rankin AH, Woolley AR (1994) Petrogenetic significance of solid carbonate inclusions in apatite of the Sukulu carbonatite, Uganda. Lithos 31:177–187
Westrich HR, Holloway JR (1981) Experimental dehydration of pargasite and calculation of its entropy and Gibbs energy. Am J Sci 281:922–934
Wyllie PJ (1966) Experimental studies of carbonatite problems: the origin and differentiation of carbonatite magmas. In: Tutle OF, Gittins J (eds) Carbonatites. Interscience, New York, pp 311–352
Wyllie PJ (1978) Peridotite-CO_2–H_2O and the low-velocity zone. Bull Volcanol 41(4):670–683
Wyllie PJ (1980) The origin of kimberlites. J Geophys Res 85 (B12): 6902–6910
Wyllie PJ (1987) Discussion of recent papers on carbonated peridotite, bearing on mantle metasomatism and magmatism. Earth Planet Sci Lett 82:391–397
Yaxley GM, Crawford AJ, Green DH (1991) Evidence for carbonatite metasomatism in spinel perodotite xenoliths from western Victoria, Australia. Ibid 107:305–317